

Supporting information for:

Highly Efficient Electrocatalytic Oxidation of Furfural to Maleic Acid over MOF-Derived MnCeOx

Xue Yuan,¹ Xin Huang,^{1} Meimin Hu,² Jinjia Liu,^{3,4*} Wenhao Guo,⁵ Yuchen Hao,⁵
Zhenting Li,⁵ Kai Zhang,⁵ Buxing Han^{6*}*

¹School of Science, China University of Geosciences, Beijing 100083, China.

²Chemical engineering institute, Inner Mongolia University of Technology, Hohhot 010051, China

³National Energy Center for Coal to Clean Fuels, Synfuels China Co., Ltd, Huairou, Beijing, 101400, China

⁴College of Chemistry and Environmental Science, Inner Mongolia Key Laboratory of Green Catalysis, Inner Mongolia Normal University, Hohhot 010022, China

⁵School of Water Resources and Environment, China University of Geosciences, Beijing 100083, China

⁶Beijing National Laboratory for Molecular Science, CAS Key Laboratory of Colloid and Interface and Thermodynamics, CAS Research/Education Center for Excellence in Molecular Sciences, Institute of Chemistry, Chinese Academy of Sciences, Beijing 100190, China.

E-mails: huangxin@cugb.edu.cn, hanbx@iccas.ac.cn

Experimental Section

Materials

Furfural (99%) and furan (98%) were purchased from Aladdin. 2-Furoic acid (98%), 2(5H)-furanone (98%), manganese(II) nitrate tetrahydrate ($\text{Mn}(\text{NO}_3)_2 \cdot 4\text{H}_2\text{O}$, 98.0%), benzene-1,3,5-tricarboxylic acid ($\text{H}_3\text{-BTC}$, 98%), and cerous (III) nitrate hexahydrate ($\text{Ce}(\text{NO}_3)_3 \cdot 6\text{H}_2\text{O}$, 99.0%) were obtained from Innochem Scientific Ltd. Toray carbon paper (CP, TGP-H-60, 19×19 cm), Nafion D-521 dispersion (5% w/w in water and 1-propanol, ≥ 0.92 meg/g exchange capacity) and Nafion N-117 membrane (0.180 mm thick, ≥ 0.90 meg/g exchange capacity) were provided Alfa Aesar China Co., Ltd. All reagents obtained from commercial sources were used without further purification.

Preparation of MnCeOx

MnCeOx was synthesized through the hydrothermal method. Typically, 0.01 mol of 1,3,5-benzenetri-carboxylic acid ($\text{H}_3\text{-BTC}$) was dissolved in 50 mL of deionized water, 0.005 mol of $\text{Mn}(\text{NO}_3)_2 \cdot 4\text{H}_2\text{O}$ and 0.005 mol of $\text{Ce}(\text{NO}_3)_3 \cdot 6\text{H}_2\text{O}$ were dissolved in 150 mL water and 200 mL of ethanol. After that, the above two solutions were mixed and stirred for 1 h, the as-obtained solution was transferred to the Teflon-coated stainless steel autoclave and maintained at 120 °C for 10 h. After cooled to room temperature, the MnCe-BTC white precipitate was washed with deionized water and ethanol by centrifugation three times. Finally, the obtained white product was dried and then carbonized in a muffle furnace at 500 °C for 2 h (at a heating rate of 5 °C /min). The obtained black powder was collected after the temperature was cooled down to room temperature.

Preparation of CeO₂ and Mn₃O₄

For comparison, the Mn_3O_4 and CeO_2 were prepared by pyrolyzing Mn-BTC and Ce-BTC. The route for the synthesis of Mn-BTC and Ce-BTC was the same as that for the preparation of MnCe-BTC except for the absence of $\text{Ce}(\text{NO}_3)_3 \cdot 6\text{H}_2\text{O}$ and $\text{Mn}(\text{NO}_3)_2 \cdot 4\text{H}_2\text{O}$, respectively. Then, the Mn-BTC or Ce-BTC were calcined at 500 °C for

2 h under Ar atmosphere. The black powders were obtained and named as Mn₃O₄ and CeO₂.

Characterization

Powder X-ray diffraction (XRD) patterns were collected on the X-ray diffractometer (Model D/MAX2500, Rigaku) with Cu-K α radiation. X-ray photoelectron spectroscopy (XPS) analysis was performed on the Thermo Scientific ESCA Lab 250Xi using 200 W monochromatic Al K α radiation, and the 500 μ m X-ray spot was used. The base pressure in the analysis chamber was about 3×10^{-10} mbar. Typically, the hydrocarbon C1s line at 284.8 eV from adventitious carbon was used for energy referencing. The morphologies of materials were characterized by a HITACHI S-4800 scanning electron microscope (SEM) and a JEOL JEM-2100F high-resolution transmission electron microscopy (HR-TEM). N₂ adsorption/desorption isotherms of the materials were measured on a Quadrasorb SI-MP system at 77 K. Before analysis, samples were allowed to outgas at 180 °C under turbomolecular vacuum pumping for a minimum of 5 h.

Linear sweep voltammetry (LSV) measurement

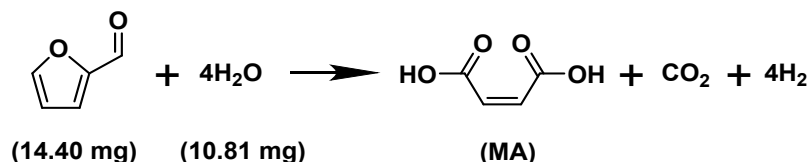
Various electrodes were firstly prepared. 2 mg of the as-prepared catalysts and 10 μ L of Nafion D-521 dispersion were dispersed in 1 mL acetone and ultrasonicated to form uniform suspension, and suitable amount of the suspension was loaded on the 1 cm \times 1 cm CP. After being dried in N₂ atmosphere, the loading of catalyst could be calculated from the weight change of the CP.

Linear sweep voltammetry (LSV) measurements were conducted in a single compartment cell with three electrodes, including a working electrode, a platinum gauze auxiliary electrode, and an Ag/AgCl reference electrode. An electrochemical workstation (CHI 660E, Shanghai CH Instruments Co., China) was employed. The LSV measurements in aqueous KHCO₃ electrolyte were carried out in a certain potential range at a sweep rate of 50 mV \cdot s⁻¹ under slight magnetic stirring.

Electrochemical oxidation of furfural to MA

The electrochemical oxidation of furfural was carried out at room temperature with a typical H-type cell, which was separated by a Nafion membrane. A typical electrochemical oxidation experiment was conducted in 15 mL of a 0.5 M KHCO₃ solution in the presence or absence of 10 mM furfural. The conversion of furfural and the yield of the corresponding products were characterized by HPLC technique. Specifically, 100 µL samples were collected from the electrolyte after reaction and then diluted with 900 µL water. After filtrated by a 0.22 µm filter, the samples were used for the HPLC analysis. The HPLC analysis was conducted on a Shimadzu Prominence Liquid Chromatograph (LC-20TA) equipped with a C18 column (Ascentis Express, 15 cm × 2.1 mm, 2.7 µm) and an ultraviolet detector. Mobile phase A was 0.1% formic acid aqueous solution adjusted to pH = ~3 with ammonium formate, and mobile phase B was acetonitrile. The flow rate was 0.3 mL/min (gradient program: 100% A for 2 min, to 20% A over 32 min, and held for 18 min). The quantification of furfural and its oxidation products were calculated based on the calibration curves obtained using standard compounds.

E-factor calculations



Total amount of reactants: 14.40 mg + 10.81 mg = 25.21 mg

Catalyst 1: MnCeO_x (MA yield = 67.4%)

Amount of final product: 11.74 mg

Amount of waste: (25.21-11.74) mg = 13.47 mg

E-Factor = Amount of waste/Amount of product = 13.47/11.74 = 1.15

Catalyst 2: CeO₂ (MA yield = 45.1%)

Amount of final product: 7.85 mg

Amount of waste: $(25.21 - 7.85) \text{ mg} = 17.36 \text{ mg}$

E-Factor = Amount of waste/Amount of product = $17.36/7.85 = 2.21$

Catalyst 3: Mn_3O_4 (MA yield = 17.4%)

Amount of final product: 3.03 mg

Amount of waste: $(25.21 - 3.03) \text{ mg} = 22.18 \text{ mg}$

E-Factor = Amount of waste/Amount of product = $22.18/3.03 = 7.32$

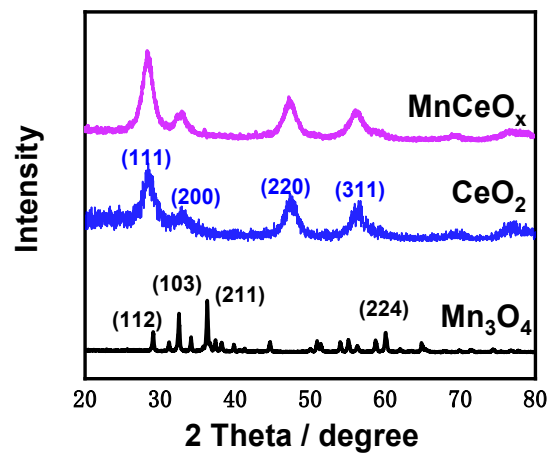


Figure S1. XRD patterns of MnCeO_x , Mn_3O_4 , and CeO_2 samples.

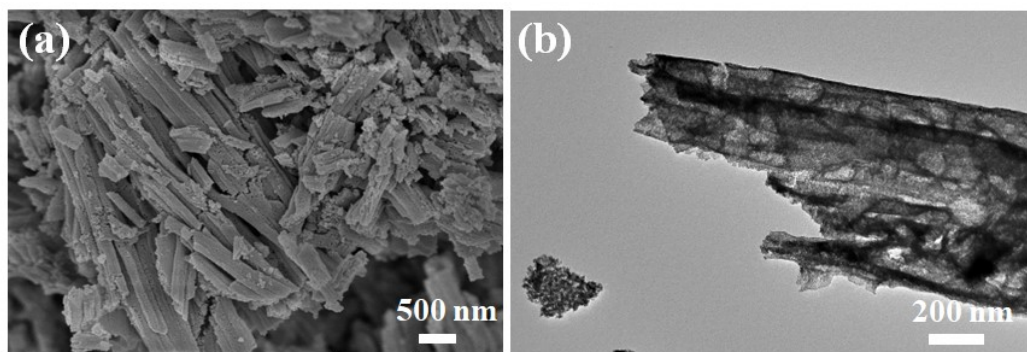


Figure S2. (a) SEM image and (b) TEM image of CeO_2 .

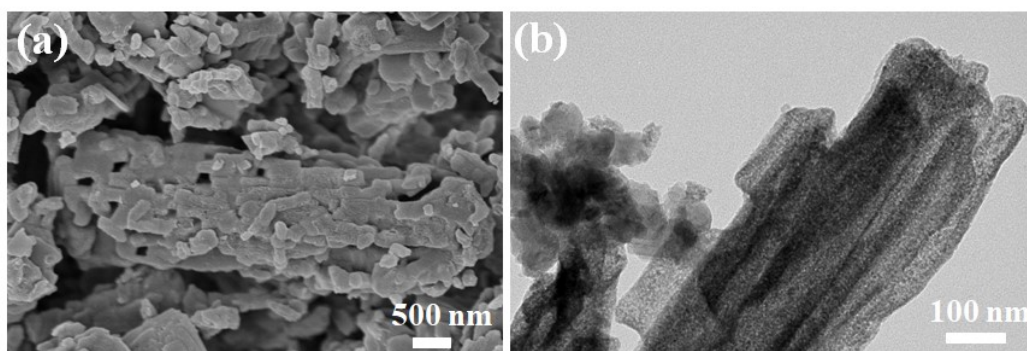


Figure S3. (a) SEM image and (b) TEM image of Mn_3O_4 .

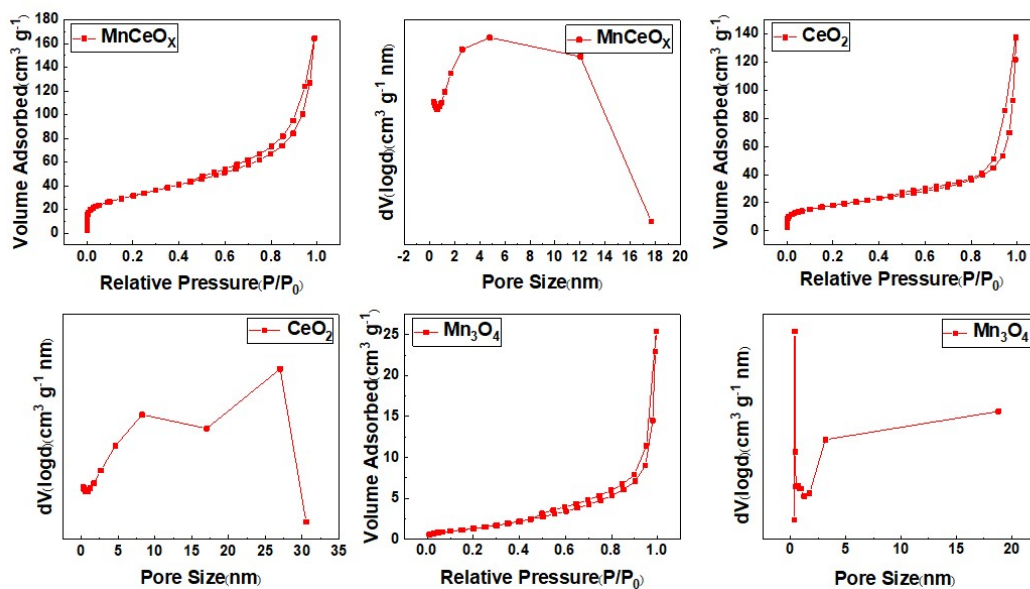


Figure S4. N₂ adsorption-desorption isotherms (77 K) of the synthesized catalysts.

Table S1. Molar ratio of Ce and Mn in MnCeO_x determined by the ICP-OES.

Mn (wt%)	Ce (wt%)	Molar ratio of Ce/Mn
11.47	67.83	2.32

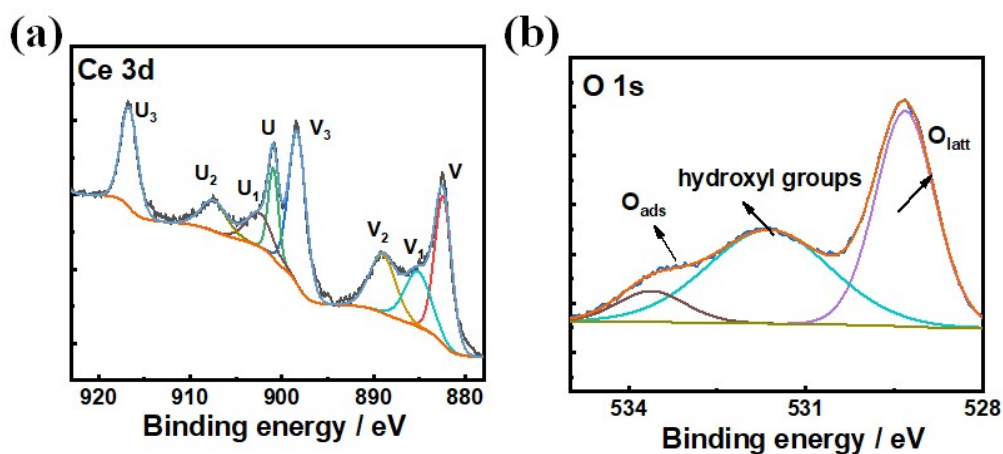


Figure S5. XPS spectra of (a) Ce 3d and (b) O 1s of CeO₂ catalysts.

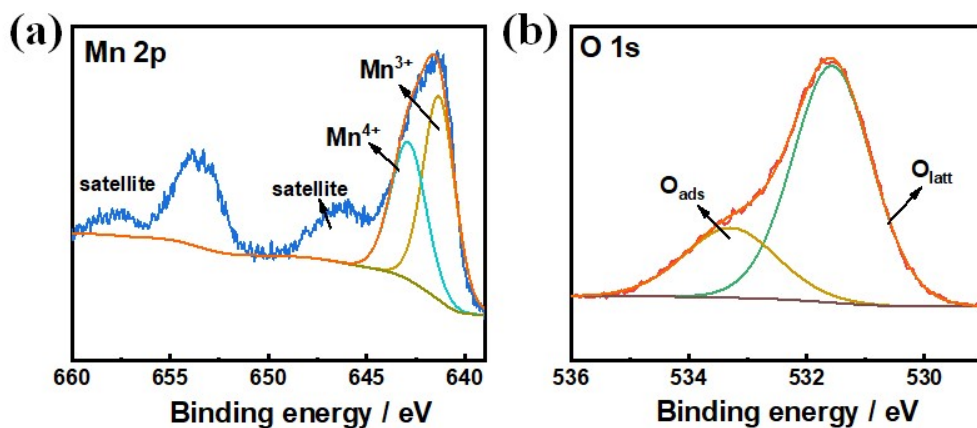


Figure S6. XPS spectra of (a) Mn 2p and (b) O 1s of Mn₃O₄ catalysts.

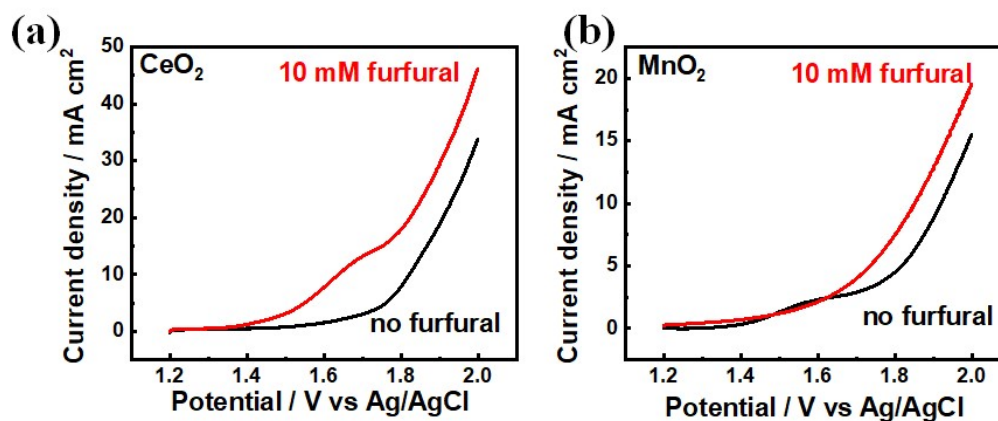


Figure S7. LSV curves of (a) CeO₂ and (b) Mn₃O₄ at a scan rate of 50 mV/s in 0.5 M aqueous KHCO₃ solution with and without furfural

Table S2. Comparison of catalytic systems to produce MA from furfural.

Catalyst	Reaction system /Electrolyte	pH	Reaction condition	MA yield	E-factor	Ref.
MnCeO _x	0.5 M KHCO ₃	8.7	1.7 V vs. Ag/AgCl	67.4%	1.15	This work
β-PbO ₂	0.5 M H ₂ SO ₄	0-1	1.8 V vs. Ag/AgCl, TEMPO	26%	4.57	1
PbO ₂	H ₂ SO ₄	1	2.0 V vs. RHE	65.1%	1.23	2
Enzyme and ACT	Photo-, electro-, biocatalysis	8.5	green LEDs (30 W), 0.8 V vs. Ag/AgCl	79%	—	3
Pb _{0.9} Bi _{0.1} O _x	0.1 M H ₂ SO ₄	2	2.2 V vs. RHE	57%	1.54	4
PdO	H ₂ SO ₄ /CH ₃ CN/H ₂ O	—	1.06 V vs. RHE	20.0%	6.24	5
Mo ₄ VO ₁₄	acetic acid	—	O ₂ 20 bar, 120°C	65%	69.81	6
VO _x /Al ₂ O ₃	O ₂	—	2.5 kPa O ₂ , 593 K	73%	—	7
Copper (II) salts with phosphomolybdic acid	Water/Tetrachloroet hane biphasic system	—	O ₂ , 20 atm, 383 K	34.5%	40.04	8
betaine hydrochloride (BHC)	Water	—	H ₂ O ₂ , 100 °C	61%	27.53	9

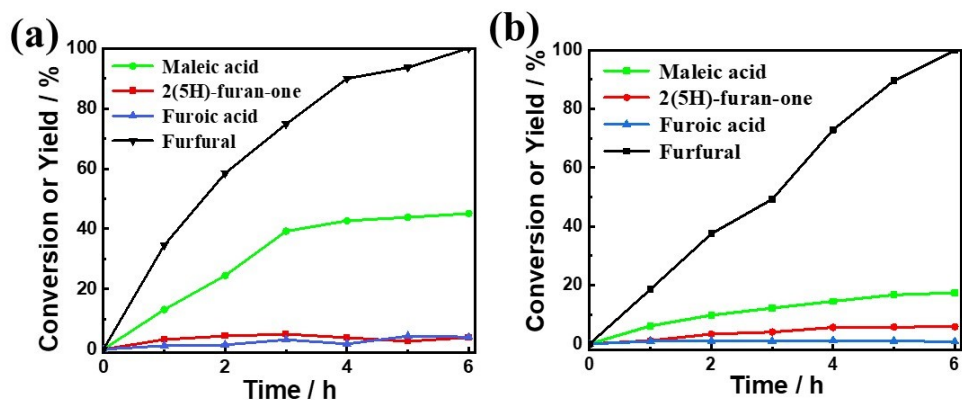


Figure S8. Conversion of furfural and yield of products at various electrolysis times at 1.7 V vs. Ag/AgCl for (a) CeO₂ and (b) Mn₃O₄.

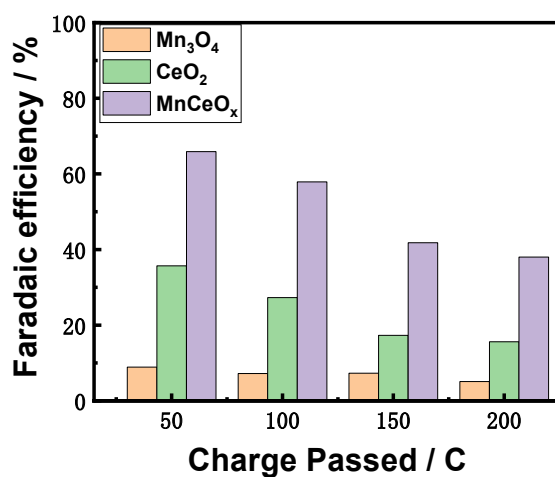


Figure S9. FE of MA over MnCeO_x, CeO₂ and Mn₃O₄.

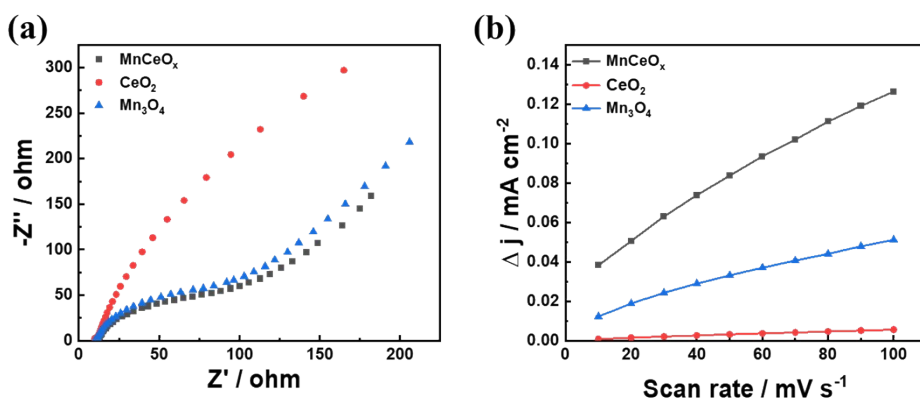


Figure S10. (a) Charging current density differences plotted against scan rates, and (b) Nyquist plots of MnCeO_x, CeO₂ and Mn₃O₄.

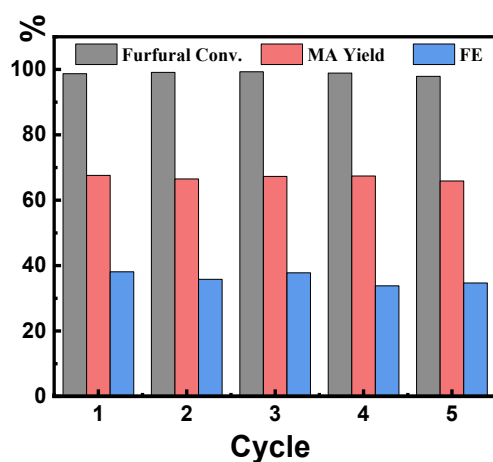


Figure S11. Reusability of MnCeOx electrode at 1.7 V vs. Ag/AgCl.

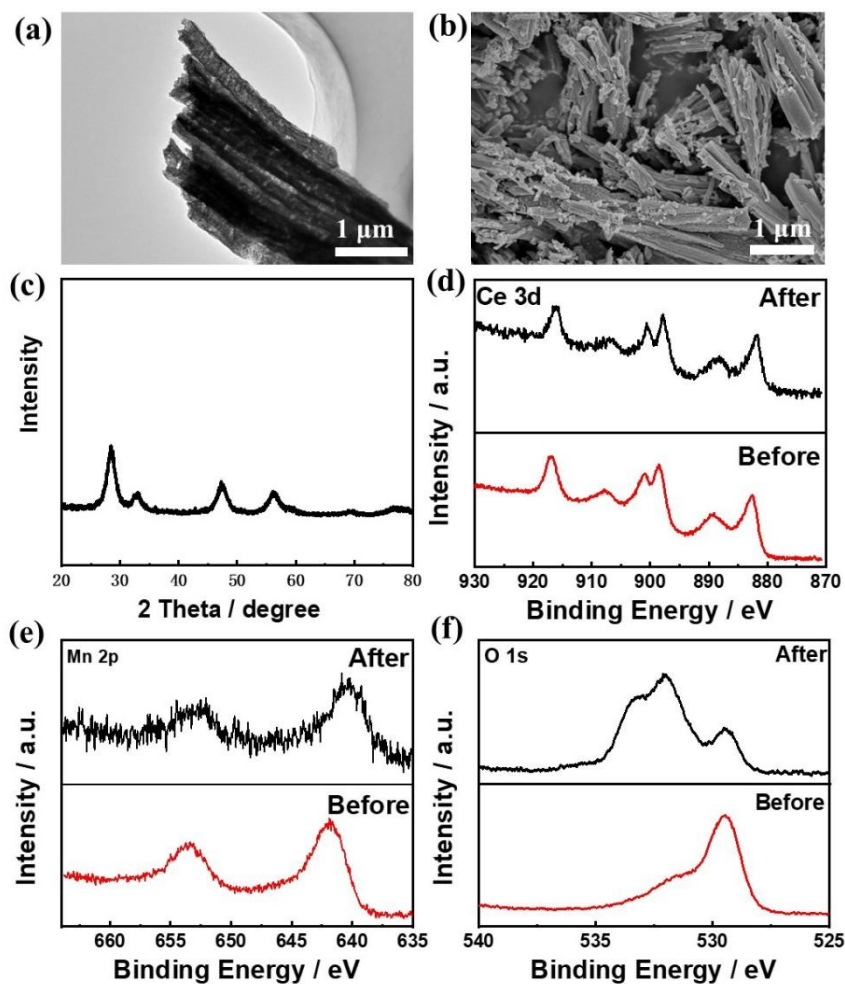
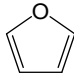
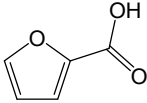
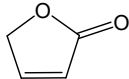
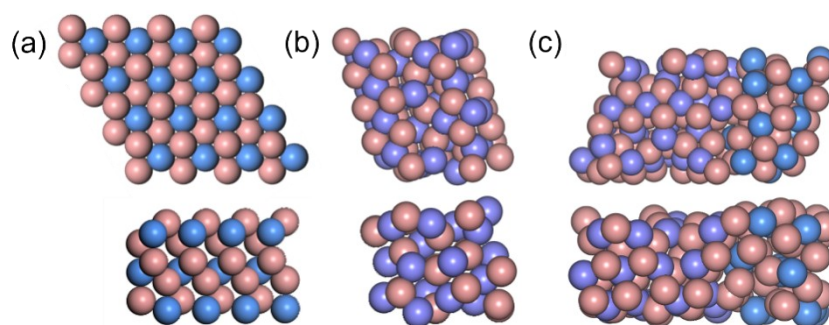
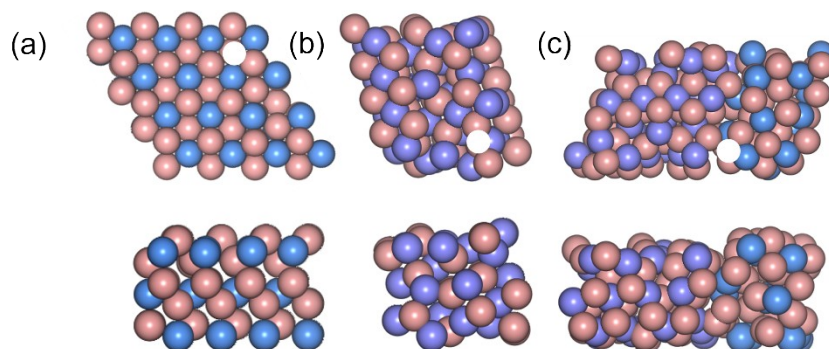


Figure S12. Characterizations of recovered MnCeOx electrode after electrolysis. (a) TEM image, (b) SEM image, (c) XRD pattern, (d) Ce 3d spectrum, (e) Mn 2p spectrum, and (f) O 1s spectrum of MnCeOx before and after electrolysis.

Table S3. Electrochemical oxidation of other reactants over the MnCeO_x.^[a]

Entry	Reactants	Conversion (%)	MA Yield (%)	Selectivity (%)
1		< 1	< 1	-
2		99.9	70.5	68.7
3		99.7	78.2	74.9

[a] Reaction conditions: applied potential, 1.7 V vs. Ag/AgCl; reactant concentration, 10 mM; 0.5 M aqueous KHCO₃ electrolyte, 15 mL; reaction time, 6 h.

**Figure S13.** The top and side views of (a) CeO₂(111), (b) Mn₃O₄(103) and (c) CeO₂(111)/Mn₃O₄(103) surfaces.**Figure S14.** The top and side views of surfaces with one oxygen vacancy, (a) CeO₂(111), (b) Mn₃O₄(103) and (c) CeO₂(111)/Mn₃O₄(103), the white circle represents the oxygen vacancy.

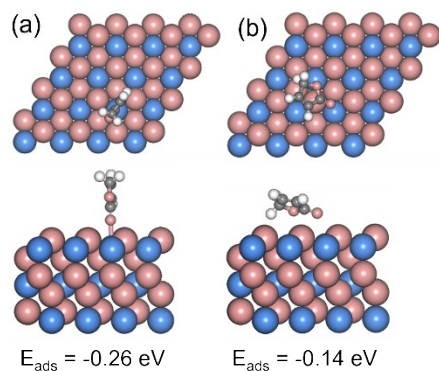


Figure S15. The top and side views of furfural adsorption configurations on $\text{CeO}_2(111)$ surface with one oxygen vacancy, (a) on Ce site, (b) on O site.

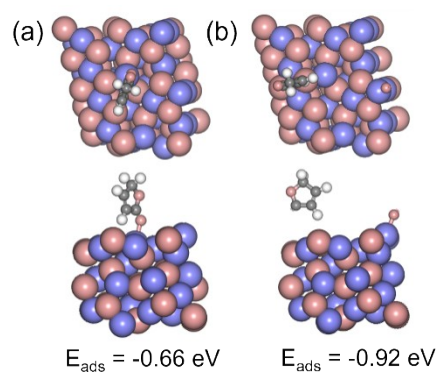


Figure S16. The top and side views of furfural adsorption configurations on $\text{Mn}_3\text{O}_4(103)$ surface with one oxygen vacancy, (a) on Mn site, (b) on O site.

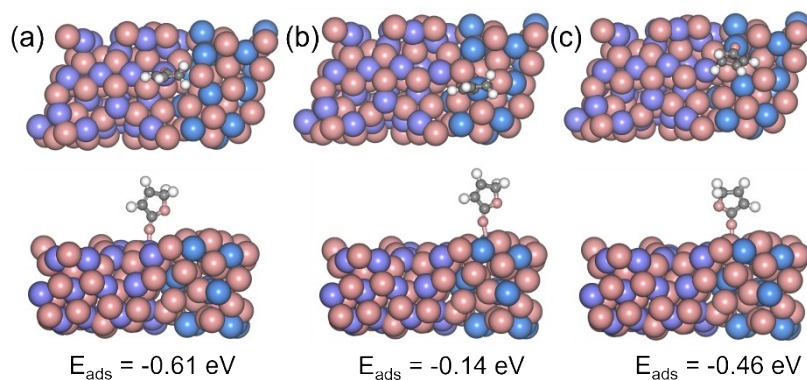


Figure S17. The top and side views of furfural adsorption configurations on $\text{CeO}_2(111)/\text{Mn}_3\text{O}_4(103)$ surface with one oxygen vacancy, (a) on Mn site, (b) on Mn site, (c) on O site.

References

1. S. Thiyagarajan, D. Franciolus, R. J. M. Bisselink, T. A. Ewing, C. G. Boeriu and J. van Haveren, *ACS Sustainable Chem. Eng.*, 2020, **8**, 10626-10632.
2. S. R. Kubota and K.-S. Choi, *ACS Sustainable Chem. Eng.*, 2018, **6**, 9596-9600.
3. G.-H. Lu, M.-H. Zong and N. Li, *ACS Catal.*, 2023, **13**, 1371-1380.
4. E. Lee, J. H. Kim, J. Choi, Y. Hong, D. Shin, H. Yun, J. Kim, G. Bak, S. Hong and Y. J. Hwang, *J. Mater. Chem. A*, 2023, **11**, 16559-16569.
5. J. Bi, Q. Zhu, W. Guo, P. Li, S. Jia, J. Liu, J. Ma, J. Zhang, Z. Liu and B. Han, *ACS Sustainable Chem. Eng.*, 2022, **10**, 8043-8050.
6. X. Li, B. Ho and Y. Zhang, *Green Chem.*, 2016, **18**, 2976-2980.
7. N. Alonso-Fagúndez, M. L. Granados, R. Mariscal and M. Ojeda, *ChemSusChem*, 2012, **5**, 1984-1990.
8. H. Guo and G. Yin, *The Journal of Physical Chemistry C*, 2011, **115**, 17516-17522.
9. N. Araji, D. D. Madjinza, G. Chatel, A. Moores, F. Jérôme and K. De Oliveira Vigier, *Green Chem.*, 2017, **19**, 98-101.